THE JOURNAL OF PHYSICAL CHEMISTRY C

Article

Cite This: J. Phys. Chem. C 2019, 123, 24156−24164

pubs.acs.org/JPCC

Atomic Sulfur Formation Mechanism on 3-Mercaptopropanoic Acid Derivative Self-Assembled Monolayers: Understanding the C−S Bond Cleavage

Julio C. Azcárate,*[,†] Natalia D. Aagaard,[†] Guillermo Zampieri,[†,‡] Eugenia Zelaya,[†] and Mariano H. Fonticelli*[,§]

[†]Centro Atómico Bariloche (CAB), Comisión Nacional de Energía Atómica − CONICET, https://www.conicet.gov.ar/

[‡]Instituto Balseiro (IB), Universidad Nacional de Cuyo (UNCuyo), Bariloche, Argentina

[§]Instituto de Investigaciones Fisicoquímica Teóricas y Aplicadas (INIFTA), Departamento de Química, Facultad de Ciencias Exactas, Universidad Nacional de La Plata (UNLP) − CONICET, https://www.conicet.gov.ar/

Supporting Information

ABSTRACT: Self-assembled monolayers (SAMs) of ω-carboxylic acid thiols are very important in the surface modification of metals, especially on gold surfaces. Indeed, the 3-mercaptopropanoic acid (MPA) and its ester or amide derivatives are widely used for SAM-based sensor design. It was already shown that MPA does not suffer C−S bond scission when adsorbed on Au. On the other hand, in this work we demonstrate that its simplest derivative, methyl 3-mercapto propionate (Me-MPA), is prone to form significant amounts of atomic sulfur when adsorbed on Au. The MPA derivatives are more sensible than MPA itself to alkaline solutions, and its SAM-based sensors will rapidly degrade given atomic sulfur. In this work, we study the simplest MPA derivative Me-MPA SAMs on preferentially oriented Au(111) surfaces by XPS and electrochemical measurements. It was found that the desulfuration of Me-MPA depends on its preparation conditions (grown from ethanol or toluene solution) and on its post-treatment with alkaline solution. In order to explain the S−C bond scission on Me-MPA SAMs, we discuss different reaction mechanisms. We concluded that the reaction mechanism involves an E1cB elimination pathway (β-elimination). This reaction mechanism also explains the desulfuration behavior of other important related molecules like L-cysteine and glutathione.

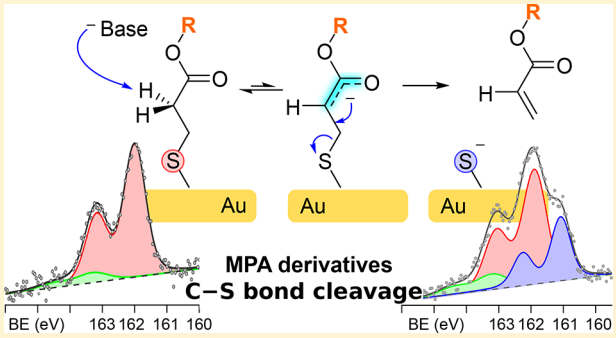

INTRODUCTION

The self-assembled monolayers (SAMs) of molecules on metals are widely studied for their interest in sensors' development, the construction of devices based on modified electrodes, and molecular electronics.[1,2] Thiols are probably the most popular substances to prepare SAMs since they allow the versatile modification of metal or semiconductor surfaces. Moreover, the ω-modification of thiols is one of the keys to solve in the "SAM engineering". Particularly important is the modification of thiols with carboxylic groups, which are easily functionalized through the formation of amides or esters, even in aqueous medium. Thus, it is of paramount importance to comprehend the surface chemistry of esters or amides of ω-carboxylic thiols. Carbodiimide derivatization provides one of the most popular and versatile methods for the covalent attachment of proteins, nucleic acids, and small organic molecules to SAMs of ω-carboxylic acid thiols. This strategy has been widely applied for the bioconjugation of Au surfaces.[3−7] The 3-mercaptopropionic acid (MPA) SAM and its derivatives, or even the very popular and commercially available dithiobis(succinimidyl propionate) (DSP, also known as Lomant's reagent), have been used as linkers to develop sensors based on bioelectrochemical electrodes,[8−11] a quartz crystal microbalance,[12] surface-enhanced resonance Raman scattering,[13] and photoluminescence.[14] The MPA derivatives were also used as building blocks for complex arrays of gold nanoparticles.[15−17]

Atomic sulfur drastically modifies the electronic properties of coinable metals (e.g., surface plasmon resonance and catalytic activity).[18] Moreover, even a very small amount of atomic sulfur can severely attenuate—or bias—the electrochemical response of a sensor that works, for example, through an impedance signal. Indeed, the quality of close-packed organic layers is a key factor to develop impedimetric sensors. As a matter of fact, very recent fundamental investigations about the responses of impedimetric aptamer biosensors reported that a variety of phenomena, not related with biomolecular interactions, drastically modify the impedance

Received: July 30, 2019
Revised: September 6, 2019
Published: September 9, 2019

DOI: 10.1021/acs.jpcc.9b07271
J. Phys. Chem. C 2019, 123, 24156−24164

response.[19] The authors covalently immobilized streptavidin to MPA SAMs on Au and subsequently attached biomolecules to build up a multilayer biosensor. In this regard, we found in the literature some evidence of the drawbacks related to the use of MPA ester derivatives to build up SAMs on Au. Based on the impedance results, it was reported that the SAMs of MPA are more efficient to block the access of a redox couple than those of DSP.[10] This is counterintuitive since the more voluminous and longer molecule should restrict more efficiently the access of the redox couple to the interface. Notably, this is not an isolated result, and a similar behavior has been independently reported elsewhere.[11] We advance that atomic sulfur can be present at considerable surface concentration in this kind of MPA-based architectures. Our interpretation may explain the lower coverage of ester moieties since its adsorption would lead to adsorbed thiolate and atomic sulfur on Au.

Commonly, some thiol SAMs present atomic sulfur as a byproduct of the adsorption due to C−S bond scission. Contrary to the idea that atomic sulfur comes from contamination,[20] it can be formed along with the SAM formation or as a consequence of thiolate degradation.[18,21] Indeed, the C−S bond breaking of alkanethiolates has been reported for many metals with distinguishing catalytic properties as Pd,[22] Ni,[21] Cu,[23] and Pt.[24] On the other hand, long-chain alkanethiols only lead to alkanethiolate species when chemisorbed on Au. On the other hand, the C−S bond breaking to lead to atomic sulfur has been reported for a representative number of molecules containing a mercapto group and another chemical functionality.[18,20,25,26] However, there is a lack of theoretical or empirical tools to predict whether a mercapto group in a molecule would lead to C−S bond scission. In a first sight, the metallic Au is not sufficiently reactive, in comparison with Pd or Pt, to promote the breakdown of the C−S bond.[27] Looking closely to the SAMs' degradation processes, there are several factors that influence the extension of a possible C−S bond breaking. Among them are the composition and structure of the substrate, the temperature, the solvent, and the chemical nature of the thiol.[23,25,28,29] Then, to understand the SAMs' degradation mechanism, many variables must be considered. More importantly, during and after C−S bond scission, the roles of the different chemical bonds in the whole thiol have to be considered. More specifically, the suitable location of additional functional groups—besides the mercapto group—has to be considered to predict if a desulfuration process is expected to occur.

Next, we discuss how the decomposition of thiomalic acid upon its adsorption on gold (both planar and nanoparticle surfaces) was rationalized in terms of reaction pathways.[18] It was claimed that the carboxylic group weakens the C−S bond in the α position with respect to a carboxylic acid group. Therefore, in a heterolytic C−S scission the carbanion can be partially stabilized by resonance charge delocalization with a carboxylic group.[18] On the contrary, for MPA SAMs atomic sulfur is not formed on Au surfaces at room temperature.[18,30] The difference in relation with the behavior of thiomalic acid can be explained considering that the C−S bond of MPA is not next to the carboxylic group, and the further carbanion could not be stabilized by charge delocalization. Up to now, the reasoning is relatively simple, and the experimental evidence supports these ideas.[18,30] On the other hand, there are systems of huge importance in applications, which demand more attention and new ideas to explain why C−S bond scission happens. Jiang et al. reported the presence of small amounts of atomic sulfur after derivatization of preformed MPA SAMs on Au surfaces.[8] As already mentioned, the derivatization of carboxylic moieties is of great importance, and MPA is one of the most popular targets.[19,31−34] For this reason, in this work we studied the atomic sulfur formation on SAMs of methyl 3-mercapto propanoate (Me-MPA). This is the simplest choice to get the essence and the rationale of the C−S bond breaking when SAMs derived from MPA—but not MPA itself—do form. We support our reasoning on experimental results taken by X-ray photoelectron spectroscopy (XPS), electrochemical characterization of the SAMs, and computational calculation. Based on the experimental data, we propose a mechanism based on the E1cB elimination reactions to explain the C−S scission for MPA derivatives SAMs. Our reasoning not only describes the behavior of MPA and Me-MPA but also provides a rational framework to describe the desulfuration of structurally related molecules—as cysteine and gluthatione—which also leads to atomic sulfur when adsorbed on Au.

EXPERIMENTAL AND CALCULATION DETAILS

Preferentially oriented Au(111) substrates were prepared by flame annealing of commercially purchased glass, coated with a gold film (Arrandee). SAMs were prepared by immersion of Au substrates in 50 μM thiol solutions overnight. After SAM preparation, the sample was carefully rinsed with fresh solvent (ethanol or toluene). Immediately before each experiment, the sample was quickly dried by N_2 gas flow. The thiols were bought from commercial sources: 3-mercapto propionic acid (MPA) from Aldrich and methyl 3-mercaptopropanoate (Me-MPA) from Acros Organics (Scheme 1). The XPS measurements were carried out by means of a SPECS Phoibos 150 spectrometer, with a monochromatized Al Kα (1486.6 eV) X-ray source. The characterizations were performed at room temperature at base pressure better than 5×10^{-10} mbar. The energy scale calibration was referenced to the Au $4f_{7/2}$ peak at 84 eV and the Fermi edge at 0 eV. Wide scan spectra and Au 4f, S 2p, C 1s, and O 1s narrow scan spectra were measured with an energy pass of 20 eV and energy step of 0.05 eV. The Au 4f region was fitted with a Doniach−Sunjic line shape where the Lorentzian width was fixed to 0.317 eV, and the asymmetry parameter was fixed to 0.052.[35] The other signals were fitted with a Voigt profile, with a Lorentzian width of 0.2 eV. Each component of the S 2p region was described by one S $2p_{3/2}$ and S $2p_{1/2}$ doublet (spin−orbit splitting of 1.18 eV, fixed area ratio 0.5, Voigt peaks of the same shape). The entire set of spectra was adjusted recursively to find the best fit. The S1 peak at 161 eV was fitted with a fixed Gaussian width of 0.6 eV, giving for the Voigt peak a full-width at half-maximum (fwhm)

Scheme 1. Chemical Structures of the Thiols Used in This Paper: 3-Mercaptopropanoic Acid (MPA) and Methyl 3-Mercaptopropanoate (Me-MPA)

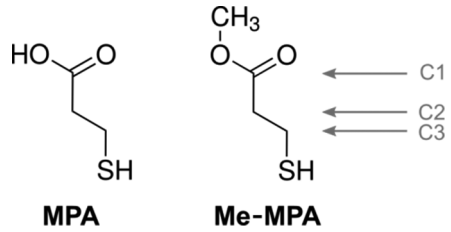

DOI: 10.1021/acs.jpcc.9b07271
J. Phys. Chem. C 2019, 123, 24156−24164

of 0.7 eV. On the other hand, the S3 at 163.3 eV was constrained to a maximum Gaussian width of 1 eV which corresponds to a fwhm of 1.1 eV for the Voigt peak. These fitting conditions are consistent with those reported elsewhere.[18] Special care has been taken in order to avoid extensive radiation damage.

The electrochemical measurements have been carried out by means of an operational amplifier potentiostat (TEQ-Argentina). A conventional three-electrode cell was used. The electrolyte, a 0.1 M NaOH aqueous solution, was deaerated with pure nitrogen before the electrochemical measurements. A saturated calomel electrode (SCE) and a large-area platinum foil were used as the reference and counter electrode, respectively. All potentials in the text are referred to the SCE scale. The real surface area of working electrodes was determined by measuring the charge needed to reduce a gold oxide monolayer, which is a two-electron process. This was done by integrating the main cathodic peak in the current−potential curves. The positive limit chosen in the cyclic voltammograms was the Burshtein minimum, as described by Hamelin et al.[36]

Density functional theory (DFT) calculations on molecular geometry optimization and vibrational frequency were performed with the hybrid-functional PBEh-3c[37] using the ORCA 4.0.1 package.[38]

RESULTS AND DISCUSSION

First, we show XPS results which demonstrate the formation of significant amounts of atomic sulfur when the ester (Me-MPA) adsorbs on Au from an ethanolic solution. On the contrary, atomic sulfur is not formed when the acid (MPA) forms SAMs on Au nor when the ester is adsorbed from a toluene solution. It is well-known that XPS is a powerful tool to interrogate the chemical nature of sulfur species by means of the S 2p region (binding energies, BEs, in the range 158−170 eV) analysis. The absolute value of the BE of the S $2p_{3/2}$ is employed to obtain information about the chemical bonding of the S to the Au surface. The S $2p_{3/2}$ core-level peak for SAMs of thiols on Au can be decomposed into three different components, S1 and S2 near 161 and 162 eV, respectively, and S3 at 163−164 eV.[18,20,30,39] The S1 component is associated with atomically adsorbed sulfur species.[18,20] The S2 component is related to S chemisorbed on the metal surface through a thiolate bond, while the S3 component has been assigned both to unbound thiol and to disulfide species.[18,30,39] We have also measured the C 1s, O 1s, and Au 4f regions for MPA and Me-MPA SAMs. Through the analysis of these data, we confirmed the presence of the carboxylic acid group in the case of MPA and the ester function in the case of Me-MPA. Finally, the Au 4f region for both MPA and Me-MPA SAMs presents spectra that are typical of alkanethiol SAMs (see Supporting Information).

For an MPA SAM (Figure 1a), the S 2p region is described by two species according to a previous report.[30] The main component, the S $2p_{3/2}$ peak at 162 eV, is assigned to thiolate (S2), and the small amount of a second broad peak at ∼163.3 eV (S3) is commonly assigned to nonbonded thiol molecules and disulfide species formed by radiation damage during X-ray exposure.[18,30,39] The relatively high amount of S3, in comparison with SAMs of dodecanethiol (see Supporting Information), is attributed to the adsorption of MPA in a second layer; i.e., molecules bond through hydrogen bonds to the SAM. Moreover, the thiolate coverage, θ_{thiolate}, resulted in 0.30 when only S2 was taken into account. This figure is

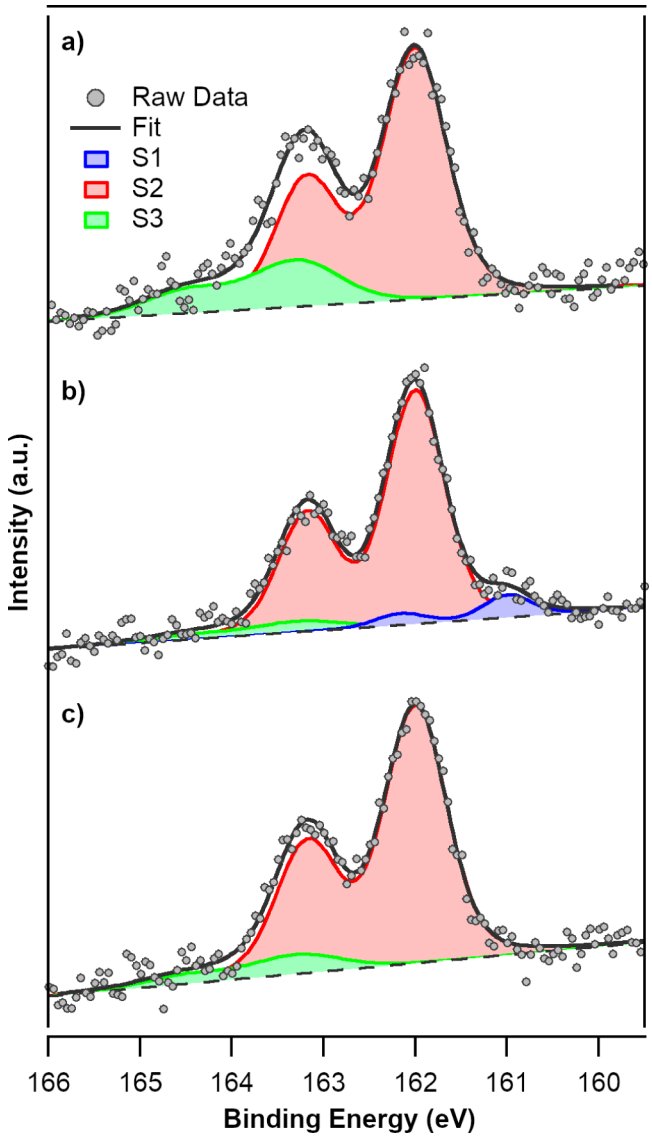

Figure 1. S 2p XPS region of (a) MPA and (b) Me-MPA SAMs prepared from ethanolic solutions and (c) Me-MPA SAM grown in toluene.

slightly smaller than those found for alkanethiolate SAMs ($\theta_{\text{thiolate}} \sim 0.33$) with low defect density but a reasonable value for a thiol with a short organic chain and a carboxylic acid moiety.[40,41] These results are in good agreement with those reported by Gonella et al.[30] Briefly, no evidence of C−S bond scission has been found for MPA SAMs.

The Me-MPA molecules adsorbed from the ethanolic solution lead to SAMs having some atomic sulfur. This is revealed by the component at 161 eV (S1) in the XP spectrum (Figure 1b). Additionally, the estimated total S coverage ($\theta_{\text{total-S}} \approx 0.31$) is comparable to that found for MPA. The S1 component corresponds to ∼8% of the whole S 2p region, which is a significant contribution. It is also interesting to note that the S3 contributions to the S 2p spectra of Me-MPA SAMs (Figures 1b and 1c) are not significant in comparison to that of MPA (Figure 1a). In fact, the ester does not have the ability to bind molecules in the second layer through hydrogen bonds, as MPA already does. In addition, although the MPA and Me-MPA are very similar molecules, the XP spectra of their SAMs are qualitatively different with regard to the

DOI: 10.1021/acs.jpcc.9b07271
J. Phys. Chem. C 2019, 123, 24156−24164

appearance of S1. Interestingly, this is not an isolated result. Indeed, the S 2p XP spectrum of Me-MPA (Figure 1b) looks pretty similar to that reported by Jiang et al. for an MPA-derivatized SAM.[8] In that work, the original MPA SAM had only the S component at 162 eV assigned to thiolate. The authors have shown that after *N*-hydroxysulfo-succinimidyl (NHSS) ester functionalization a shoulder at 161 eV developed. In other words, the atomic sulfur appears after ester formation on the preformed MPA SAM.

The spectrum in Figure 1c shows XPS data of a Me-MPA SAM formed from toluene solution. The striking aspect is the absence of the S1 component. It is remarkable that just changing the solvent leads to a qualitatively different molecular overlayer. Then, we found a way to build-up Me-MPA SAMs that are free from atomic sulfur. However, we will show that the Me-MPA SAMs grown in toluene are prone to form atomic sulfur.

There are a couple of further remarks with regard to the possible origin of atomic sulfur on Au surfaces. First, it is already known that thiolate SAMs are sensitive to X-ray irradiation, which can lead to the atomic sulfur formation.[30,42] Under the current experimental conditions, neither MPA nor Me-MPA SAMs suffered excessive radiation damage, as the 161 eV S 2p component is absent in the SAMs of Figures 1a and 1c. Then, we can rule out the radiation damage as the source of atomic sulfur in the Me-MPA SAM grown in ethanol. Second, the 161 eV component in Figure 1b does not come from contaminants in the Me-MPA reagent since otherwise this contamination would also lead to atomic sulfur for the SAMs grown in toluene.

It has been extensively reported that the chemical nature of the sulfur species and the adsorption states of the thiols can be characterized from peak potentials, E_p, in electrochemical reductive desorption runs. In the following, we present and discuss the reductive desorption of MPA and Me-MPA SAMs grown from ethanolic solutions and of Me-MPA SAMs prepared in toluene (Figure 2). Each sample has been carefully rinsed with the corresponding organic solvent and dried under a nitrogen stream. Then, the samples were immersed in 0.1 M NaOH aqueous solution to perform electrochemical analysis. The reductive desorption curve of a MPA SAM on preferentially oriented Au(111) shows a peak at −0.78 V (Figure 2, curve a). This E_p is consistent with a thiolate SAM of this short-chained carboxylic acid[41] but not with sulfur moieties (neither atomic sulfur nor S_n species).[43] The charge density (Q_{desor} = 73 μC cm^{-2}) associated with this peak—calculated after the consideration of the contribution from double-layer charging—is compatible with a dense SAM of thiolate species.[44] In some of the previous studies on the electrochemical desorption of MPA from preferred oriented Au(111), a more negative wave (E_p = −1.07 V) has been reported, which was attributed to desorption from stepped sites.[45] This might be the reason why this peak is not ever-present in careful studies by Kakiuchi et al. In fact, while it is clearly distinguished in a desorption curve recorded using 0.5 M KOH,[46] it is not present when NaOH was used as the electrolyte.[41] Briefly, we found that the electrochemical behavior of MPA on preferentially oriented Au(111) agrees with previous reports and shows that only thiolate species desorb from this surface. Figure 2 (curve b) shows a representative electrodesorption curve of a Me-MPA SAM grown from an ethanolic solution. Note that there are some similarities in the voltammetric characteristics of the

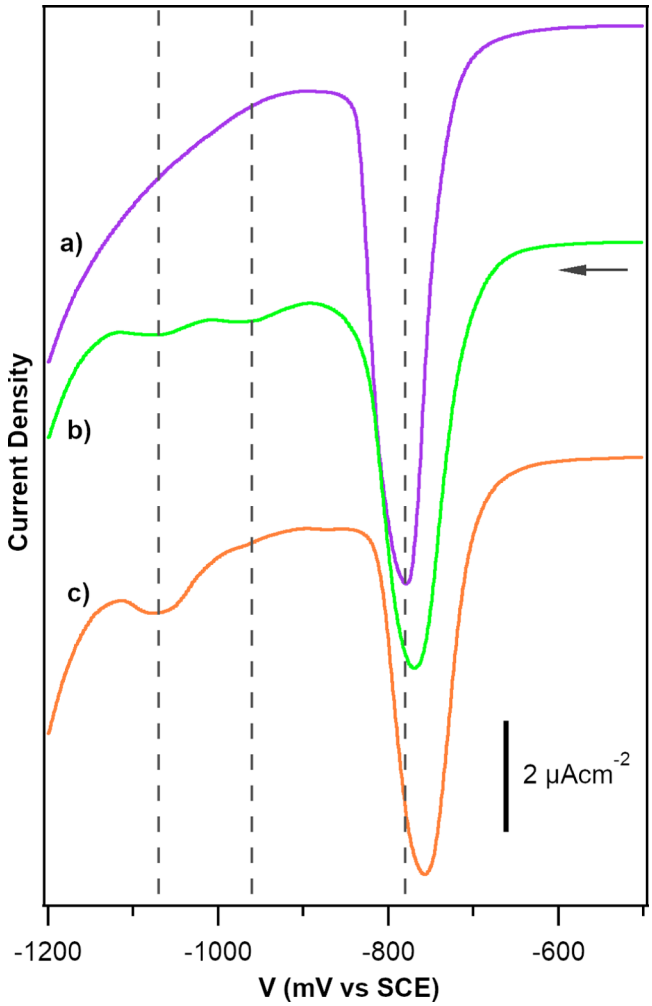

Figure 2. Electrodesorption curves of (a) MPA SAM grown in ethanol, (b) Me-MPA SAM grown in ethanol, and (c) Me-MPA SAM grown in toluene. The arrow emphasizes that the potential is scanned in the negative direction. Electrolyte: 0.1 M NaOH aqueous solution. Scan rate: ν = 0.010 V s^{-1}.

desorption curves described so far. As already reported, the peak potential associated with the thiolate desorption is slightly higher (E_p = −0.77 V) for Me-MPA than for MPA,[34] and the charge density of this peak is just less (Q_{desor} = 72 μC cm^{-2}) than that found for MPA. Up to now, we can state that the thiolate coverage is comparable to that expected for a regular SAM. Besides this apparent likeness, the Me-MPA desorption curve is qualitatively different with regard to the appearance of a signal (E_p = −0.95 V) associated with atomic sulfur. Then, the presence of atomic sulfur, which was previously associated with the S 2$p_{3/2}$ at 161 eV, in the Me-MPA SAMs is confirmed. The last signal in the curve that deserves attention is a hump (E_p = −1.07 V) that is associated with thiolate[47] and/or atomic sulfur[48] at/from step edges. Then, as in previous reports,[18,49] the usefulness of reductive desorption in combination with XPS data to assert the chemical nature of the sulfur species is confirmed. In few words, the Me-MPA is mainly composed of thiolate moieties, but significant amounts of atomic sulfur have been observed both by XPS and electrochemical measurements.

Our results are relevant to analyze previous reports on SAMs of MPA derivatives. The appearance of negative current

DOI: 10.1021/acs.jpcc.9b07271
J. Phys. Chem. C 2019, 123, 24156−24164

contribution in the potential range -1 V < E < -0.87 V vs SCE for the electrochemical desorption of DSP (an MPA derivative) was attributed to surface heterogeneity.[6] On the contrary, we consider that it could have been assigned to atomic sulfur. Moreover, in recent studies about DSP adsorption on Au, the S 2p XPS region has been fitted with just one doublet at 162 eV.[6,7] However, the shape of the spectra is compatible with an additional doublet at 161 eV.

In the case of the Me-MPA SAMs grown from a toluene solution (Figure 2c), we detected a positive potential shift of the thiolate peak (E_p = -0.76 V), a small hump in the region ascribed to atomic sulfur reduction (-0.95 V), and a marked peak for thiolate and/or sulfur desorption from step edges (E_p = -1.07 V). The presence of atomic sulfur in this sample is apparently contradictory with the XPS results, where the corresponding signal was not found (no S $2p_{3/2}$ component at 161 eV). However, we speculate that this small amount of atomic sulfur is formed when the already formed SAM was in contact with the electrolyte. We will go back to this point below.

We observed some variability in the electrochemical response of the Me-MPA monolayers, which we attribute to a few different aspects. First, in order to get better resolution in the reductive desorption processes we used a low scan rate (ν = 0.010 V s^{-1}). This can allow resolving features that otherwise would be hardly discriminated.[50,51] Second, there are subtle differences in the microstructure of the gold surface, and the impact of such differences on the nucleation and growth of the adlayers can lead to significant differences in the electrodesorption curves. Lastly, and more importantly, the basic electrolyte can induce further C−S bond scission in the SAMs prepared in ethanol and can also lead to small amounts of atomic S in the Me-MPA monolayers grown in a toluene solution.

It is interesting to further discuss the characterization results from XPS and electrochemistry of the Me-MPA SAMs grown in toluene. The electrodesorption curve in Figure 2c shows a small hump at -0.95 V, which suggests the desorption of atomic sulfur. Also, the increase of the signal at E_p = -1.07 V could be associated with a greater amount of atomic sulfur and/or thiolate at step-edges. However, the atomic sulfur is absent in the as-prepared SAMs according the XPS data (Figure 1c). We consider that when this SAM was in contact with the NaOH 0.1 M aqueous solution the Me-MPA suffered a considerable change; i.e., C−S bond cleavage was induced. To test this, we performed XPS measurements for SAMs of Me-MPA grown in toluene, which after being rinsed with pure toluene and dried under a nitrogen stream were treated with 0.1 M NaOH. Figure 3 shows the S 2p region XP spectra of SAMs immersed in aqueous NaOH for 30 min and 4 h. For both samples the presence of the peak at 161 eV is clear. Noticeably, the component assigned to atomic sulfur increases drastically with the exposure time (~7% after 30 min of NaOH treatment and ~30% after 4 h). The electrochemical data of the SAMs treated with NaOH also showed a remarkable increase in the amount of atomic sulfur (see Supporting Information Figure S4). Indeed, SAM degradation can also explain the positive E_p shift for thiolate desorption observed in Figure 2c).

To get insight into the mechanism/s involved in atomic sulfur formation we first discuss the homolytic and the heterolytic scission of the C−S bond. The formation of radicals (by a homolytic pathway) should be equally likely for both of

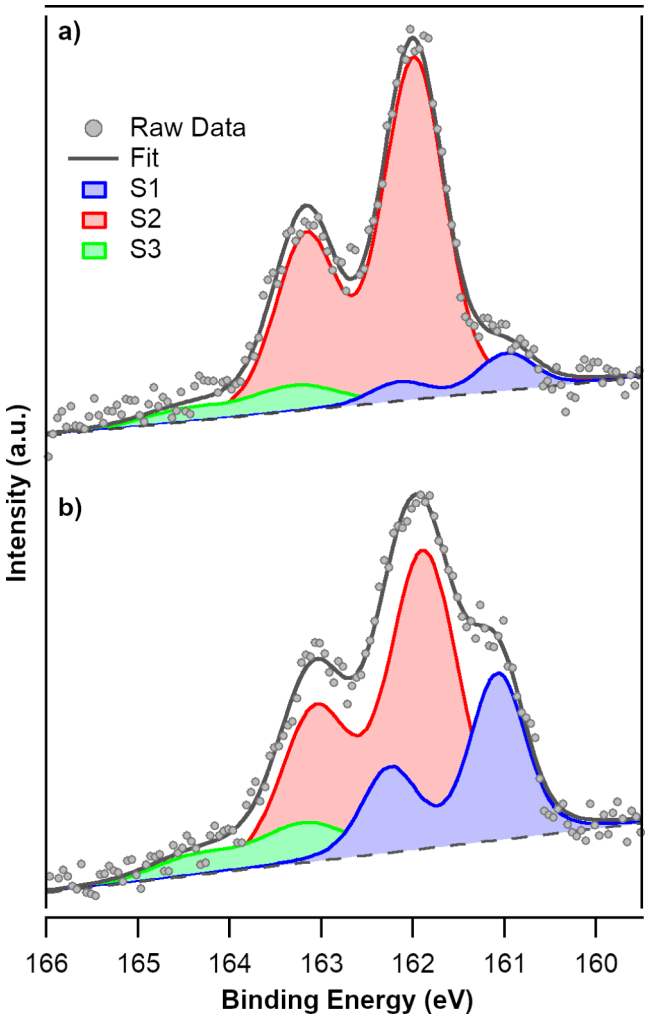

Figure 3. S 2p region XPS of Me-MPA SAMs prepared from toluene solution, after their treatment with 0.1 M NaOH aqueous solution for (a) 30 min and (b) 4 h.

the studied thiols, MPA and Me-MPA. Since the SAMs of MPA do not form atomic sulfur, those of Me-MPA should not experience the breaking of the C−S bond in this way. Indeed, for both molecules, carbon radicals in C3 are unlikely to be stabilized. Then, we consider that the heterolytic C−S bond breaking would be more probable. Next, we consider that neither carbocations nor carbanion in C3 could be stabilized because a net charge in C3 leads to highly energetic and unlikely intermediates. Therefore, we do not propose a direct mechanism in which the first step involves the C−S scission to form charged species, as it would happen in an E1 reaction.[52,53] Moreover, the results from XPS and electrochemistry show that a base is necessary to promote the C−S scission. In this regard, the E2 elimination reaction mechanism[52,53] was also ruled out for two reasons. First, the requisite of a strong base needed to abstract the H is not fulfilled by ethanol, which can be considered just as a weak Lewis base. Second, the geometrical condition for an E2 elimination (H and S in adjacent carbons, C2 and C3, in antiperiplanar confirmation) would not be achieved for standing-up molecules in a dense SAM. Therefore, after having considered different reaction mechanisms, we propose an E1cB elimination.[52] The requirement of relatively acidic hydrogen is satisfied by the H neighbors to the C═O moieties (H in C2), which is slightly

DOI: 10.1021/acs.jpcc.9b07271
J. Phys. Chem. C 2019, 123, 24156−24164

more acidic than other H in the adsorbed Me-MPA. In the first step a base withdraws the H in C2, forming a carbanion (Scheme 2). Note that, as the negative charge of the carbanion

Scheme 2. E1cB Reaction Mechanism for C−S Cleavage on the Au Surface

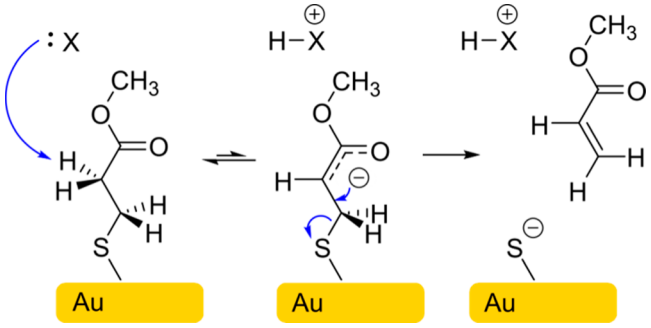

is in α position with respect to the ester group, the carbanion stability is significantly enhanced.[52] Also, after the proton transfer, a significant redistribution of electron density in the adsorbed molecule occurs. While the C2 atom has a tetrahedral (sp^3) configuration in the Me-MPA, it is flat (sp^2) in the carbanion because it is stabilized by electron delocalization.[52] It is important to note that this mechanism, which involves a negatively charged intermediate, occurs with greater probability in polar media (ethanol or aqueous solution) than in a nonpolar one (toluene solution).[53]

The intermediate can lead to atomic sulfur on gold and a methyl acrylate molecule after electron rearrangement (β-elimination). The electronic reorganization can be described considering that the negative charge relays in an orbital perpendicular to the sp^2 plane, which overlaps with the σ^*_{CS} molecular orbital, promoting the C−S bond scission. Moreover, the S bond to Au is a better leaving group than S itself because the Au surface can act as an efficient electron drain (eventually, as an electron source). When the adsorbates are in their standing-up configuration, the antibonding (empty) molecular orbital σ^*_{CS} is expected to be oriented toward the gold surface, interacting with their electrons. Moreover, additional experiments described below and DFT calculations of Me-MPA molecules and their derived carbanions show that the C−S bond scission is not plausible for nonadsorbed species.

We performed DFT calculation on molecular geometry optimization and vibrational frequency analysis for the neutral free molecule Me-MPA and the derived carbanion in C2. The first interesting result to highlight is that the vibrational frequency associated with the C−S bond stretching for the carbanion in C2 (456.4 cm^{-1}) is lower than that for the neutral molecule (725.46 cm^{-1}) in vacuum. This result is consistent with a weaker C−S bond for the carbanion than the neutral molecule. In other words, when the H in C2 is taken away, leading to a carbanion, the C−S bond is weakened. However, the energies associated with the excitation of the C−S stretching mode are higher than the thermal energy. This supports the idea that no homolytic rupture would occur in alkaline solution. Furthermore, it is expected that both species would be stable in the homogeneous phases (i.e., the ethanolic and toluene solutions).

To support the idea that a base does not induce the C−S scission in solution, but it does when Me-MPA is adsorbed, we carried out additional experiments. We alkalinized the ethanolic solution of this thiol with NaOH before the SAM preparation. We assay two different concentrations of NaOH with molar ratios of 10× and 1000× with respect to Me-MPA (i.e., 500 μM in NaOH for 10× and 50 mM for 1000× , which is close to saturation). It is important to stress that for these samples the NaOH is present along with the SAM formation. With 10× of NaOH the amount of atomic sulfur found in the XPS spectrum is quite similar to that found for the ethanolic solution (~7% of total S 2p XPS signal), and with 1000× of NaOH, the atomic sulfur rises to ~11%. It is important to note that the total sulfur surface coverage for the 1000× of NaOH sample is $\theta \approx 0.34$. From these results, we can rule out the extensive decomposition of the Me-MPA molecule in solution. Indeed, the amount of atomic sulfur found using the alkalinized thiol solution is comparable to the figure for preformed SAMs after NaOH treatment. These results confirm that C−S scission promoted by a base only occurs when Me-MPA molecules are adsorbed on Au, but it does not happen in the whole solution.

The proposed mechanisms also explain the absence of atomic sulfur on MPA SAMs. The carboxylic H is more acidic than the H in C2. Then, for MPA the interaction between H in C2 with ethanol or water molecules (bases) is negligible in comparison to that of H of the carboxylic acid group. With regards to the reactivity of molecules structurally related to those studied in this paper, it is remarkable that the tendency to enolization of a carboxylic acid group is likely to be very small compared to that of a carboxylic ester group. However, if instead of the carboxylic acid an ester or amide function is considered, there is an increase in the tendency toward enol formation with the hydrogen of the α carbon atom. In other words, the difference in reactivity between MPA and Me-MPA is well justified according to their tendency to adopt their enolic forms. Additionally, the qualitatively different behavior in the polar and nonpolar solvents is consistent with the likeliness of the E1cB elimination to occur in polar solvents. Then, we provide a successful explanation for the phenomena described in this work. Furthermore, the proposed mechanism is probably useful to explain the decomposition of MPA when it was esterified[8] and also to rationalize the presence of atomic sulfur in L-cysteine SAMs on Au.[20] More importantly, the scheme reaction would explain the fact that glutathione desulfurization only progresses when it is chemisorbed on the Au surface, and it is enhanced by an alkaline media.[49]

CONCLUSIONS

We have studied the desulfuration of the simplest derivative of 3-mercaptopropionic acid (MPA)—methyl 3-mercaptopropanoate (Me-MPA)—when it is adsorbed on Au(111) from ethanolic or toluene solutions. X-ray photoelectron spectroscopy and electrochemical desorption experiments showed that small amounts of atomic sulfur were formed for Me-MPA SAMs grown in ethanol. Meanwhile, those Me-MPA SAMs built-up in toluene are composed just by thiolate species. Additionally, we have demonstrated that the alkaline medium induces the C−S bond scission in Me-MPA SAMs. Although toluene has been an appropriate solvent to carry out the self-assembly process, the Me-MPA SAMs are prone to suffer desulfuration to a significant extent. This represents a serious objection to the use of MPA as a linker in some of the already spread applications and fundamental studies.

DOI: 10.1021/acs.jpcc.9b07271
J. Phys. Chem. C 2019, 123, 24156−24164

Looking forward to the detailed description of the C−S bond cleavage, we rationalize the experimental results into the frame of a β-elimination reaction. Indeed, we found three experimental features which strongly favor the E1cB mechanism. First, a relatively weak base (ethanol) is strong enough to enhance the Me-MPA desulfuration. Second, the E1cB mechanism does not require special geometrical configurations to progress. Then, the reaction can really progress in a dense SAM, where the Me-MPA should have partially lost some of their intramolecular degrees of freedom. Lastly, the C−S bond scission was benefited by a polar-protic solvent, ethanol, and suppressed by toluene. Briefly, all these experimental facts are consistent with an E1cB. Accordingly, the E1cB is a plausible mechanism that describes our experimental results.

It is remarkable that we could only discern the true chemical nature of the adsorbates through a critical analysis of XPS and electrochemical characterization. Even more, it was the combination of two independent techniques that allowed us to decide which of the mechanisms is the most likely.

Finally, we would like to point out that our approach could be useful to understand the desulfuration of structurally related molecules when they form SAMs on Au. Indeed, the E1cB mechanism satisfactorily explains the reported behavior for glutathione and cysteine, which also leads to atomic sulfur as a coadsorbate.[20,49]

■ ASSOCIATED CONTENT

Supporting Information

The Supporting Information is available free of charge on the ACS Publications website at DOI: 10.1021/acs.jpcc.9b07271.

S 2p region XP spectrum of a dodecanethiol SAM on the preferentially oriented Au(111) substrate, description on surface coverage calculation from XPS data, O 1s, C 1s, and Au 4f XP spectra, and electrochemical data on the strong effect of NaOH over the integrity and composition of Me-MPA SAMs (PDF)

■ AUTHOR INFORMATION

Corresponding Authors

*J.C.A. E-mail: jcazcarate@cab.cnea.gov.ar. Phone: +54 294 444 5147. Web: http://fisica.cab.cnea.gov.ar/metales.

*M.H.F. E-mail: mfonti@inifta.unlp.edu.ar. Phone: +54 221 425 7430. Web: http://nano.quimica.unlp.edu.ar.

ORCID

Julio C. Azcárate: 0000-0002-1114-4611

Eugenia Zelaya: 0000-0001-7664-8936

Mariano H. Fonticelli: 0000-0003-1739-9620

Author Contributions

The manuscript was written through the contributions of all authors. All authors have given approval to the final version of the manuscript.

Notes

The authors declare no competing financial interest.

■ ACKNOWLEDGMENTS

The authors thank Comisión Nacional de Energía Atómica (CNEA) and the Consejo Nacional de Investigaciones Científicas y Técnicas (CONICET). J.C.A., G.Z., E.Z., and M.H.F. are research members of CONICET. N.D.A. is a CONICET fellow and Ph.D. student of "Facultad de Ciencias Exactas, Universidad Nacional de La Plata (UNLP)". This work was supported in part by CONICET (PIP 0333), ANPCyT (PICT 2017-4519), Universidad Nacional de La Plata (UNLP X786) of Argentina, and Universidad Nacional de Cuyo. The authors would like to thank Dr. Agustín Pico for his help with some experimental aspects.

■ REFERENCES

(1) Love, J. C.; Estroff, L. A.; Kriebel, J. K.; Nuzzo, R. G.; Whitesides, G. M. Self-Assembled Monolayers of Thiolates on Metals as a Form of Nanotechnology. *Chem. Rev.* **2005**, *105*, 1103−1170.

(2) Bürgi, T. Properties of the Gold−sulphur Interface: From Self-Assembled Monolayers to Clusters. *Nanoscale* **2015**, *7*, 15553−15567.

(3) Liu, L.; Li, S.; Liu, L.; Deng, D.; Xia, N. Simple, Sensitive and Selective Detection of Dopamine Using Dithiobis-(succinimidylpropionate)-Modified Gold Nanoparticles as Colorimetric Probes. *Analyst* **2012**, *137*, 3794.

(4) Gu, H.; Liu, Y.; Ren, T.; Xia, W.; Guo, Y.; Shi, G. An Electrochemical Biosensor Based on Double Molecular Recognition for Selective Monitoring of Cerebral Dopamine Dynamics at 4 min Interval. *Sens. Actuators, B* **2019**, *287*, 356−363.

(5) Arya, S. K.; Chornokur, G.; Venugopal, M.; Bhansali, S. Dithiobis(succinimidyl Propionate) Modified Gold Microarray Electrode Based Electrochemical Immunosensor for Ultrasensitive Detection of Cortisol. *Biosens. Bioelectron.* **2010**, *25*, 2296−2301.

(6) Lim, C. Y.; Owens, N. A.; Wampler, R. D.; Ying, Y.; Granger, J. H.; Porter, M. D.; Takahashi, M.; Shimazu, K. Succinimidyl Ester Surface Chemistry: Implications of the Competition between Aminolysis and Hydrolysis on Covalent Protein Immobilization. *Langmuir* **2014**, *30*, 12868−12878.

(7) Ataman Sadık, D.; Eksi-Kocak, H.; Ertaş, G.; Boyacı, İ. H.; Mutlu, M. Mixed-Monolayer of N-Hydroxysuccinimide-Terminated Cross-Linker and Short Alkanethiol to Improve the Efficiency of Biomolecule Binding for Biosensing. *Surf. Interface Anal.* **2018**, *50*, 866−878.

(8) Jiang, L.; Glidle, A.; Griffith, A.; McNeil, C. J.; Cooper, J. M. Characterising the Formation of a Bioelectrochemical Interface at a Self-Assembled Monolayer Using X-Ray Photoelectron Spectroscopy. *Bioelectrochem. Bioenerg.* **1997**, *42*, 15−23.

(9) Claussen, J. C.; Wickner, M. M.; Fisher, T. S.; Porterfield, D. M. Transforming the Fabrication and Biofunctionalization of Gold Nanoelectrode Arrays into Versatile Electrochemical Glucose Biosensors. *ACS Appl. Mater. Interfaces* **2011**, *3*, 1765−1770.

(10) Mena, M. L.; Carralero, V.; González-Cortés, A.; Yáñez-Sedeño, P.; Pingarrón, J. M. Laccase Biosensor Based on N-Succinimidyl-3-Thiopropionate-Functionalized Gold Electrodes. *Electroanalysis* **2005**, *17*, 2147−2155.

(11) Im, J.-E.; Han, J.-A.; Kim, B. K.; Han, J. H.; Park, T. S.; Hwang, S.; In Cho, S.; Lee, W.-Y.; Kim, Y.-R. Electrochemical Detection of Estrogen Hormone by Immobilized Estrogen Receptor on Au Electrode. *Surf. Coat. Technol.* **2010**, *205*, S275−S278.

(12) Buchatip, S.; Ananthanawat, C.; Sithigorngul, P.; Sangvanich, P.; Rengpipat, S.; Hoven, V. P. Detection of the Shrimp Pathogenic Bacteria, Vibrio Harveyi, by a Quartz Crystal Microbalance-Specific Antibody Based Sensor. *Sens. Actuators, B* **2010**, *145*, 259−264.

(13) Owens, N. A.; Pinter, A.; Porter, M. D. Surface-Enhanced Resonance Raman Scattering for the Sensitive Detection of a Tuberculosis Biomarker in Human Serum. *J. Raman Spectrosc.* **2019**, *50*, 15−25.

(14) Singh, P.; Prabhune, A. A.; Tripathi, C. S. P.; Guin, D. Water-Soluble Photoluminescence On−Off−On Probe for Speedy and Selective Detection of Fluoride Ions. *ACS Sustainable Chem. Eng.* **2017**, *5*, 982−987.

(15) Sergeyeva, T. A.; Piletsky, S. A.; Panasyuk, T. L.; El'skaya, A. V.; Brovko, A. A.; Slinchenko, E. A.; Sergeeva, L. M. Conductimetric Sensor for Atrazine Detection Based on Molecularly Imprinted Polymer Membranes. *Analyst* **1999**, *124*, 331−334.

DOI: 10.1021/acs.jpcc.9b07271
J. Phys. Chem. C 2019, 123, 24156−24164

(16) Arita, T.; Yoshimura, T.; Adschiri, T. Size Exclusion Chromatography of Quantum Dots by Utilizing Nanoparticle Repelling Surface of Concentrated Polymer Brush. *Nanoscale* **2010**, *2*, 1467.
(17) Paez, J. I.; Coronado, E. A.; Strumia, M. C. Preparation of Controlled Gold Nanoparticle Aggregates Using a Dendronization Strategy. *J. Colloid Interface Sci.* **2012**, *384*, 10.
(18) Azcárate, J. C.; Floridia Addato, M. A.; Rubert, A.; Corthey, G.; Kürten Moreno, G. S.; Benítez, G.; Zelaya, E.; Salvarezza, R. C.; Fonticelli, M. H. Surface Chemistry of Thiomalic Acid Adsorption on Planar Gold and Gold Nanoparticles. *Langmuir* **2014**, *30*, 1820−1826.
(19) Ho, L. S. J.; Limson, J. L.; Fogel, R. Certain Methods of Electrode Pretreatment Create Misleading Responses in Impedimetric Aptamer Biosensors. *ACS Omega* **2019**, *4*, 5839−5847.
(20) Cavalleri, O.; Gonella, G.; Terreni, S.; Vignolo, M.; Pelori, P.; Floreano, L.; Morgante, A.; Canepa, M.; Rolandi, R. High Resolution XPS of the S 2p Core Level Region of the L-Cysteine/gold Interface. *J. Phys.: Condens. Matter* **2004**, *16*, S2477−S2482.
(21) Blobner, F.; Abufager, P. N.; Han, R.; Bauer, J.; Duncan, D. A.; Maurer, R. J.; Reuter, K.; Feulner, P.; Allegretti, F. Thiolate-Bonded Self-Assembled Monolayers on Ni(111): Bonding Strength, Structure, and Stability. *J. Phys. Chem. C* **2015**, *119*, 15455−15468.
(22) Corthey, G.; Rubert, A. A.; Benitez, G. A.; Fonticelli, M. H.; Salvarezza, R. C. Electrochemical and X-Ray Photoelectron Spectroscopy Characterization of Alkanethiols Adsorbed on Palladium Surfaces. *J. Phys. Chem. C* **2009**, *113*, 6735−6742.
(23) Rechmann, J.; Krzywiecki, M.; Erbe, A. Carbon−Sulfur Bond Cleavage During Adsorption of Octadecane Thiol to Copper in Ethanol. *Langmuir* **2019**, *35*, 6888−6897.
(24) Floridia Addato, M. A.; Rubert, A. A.; Benítez, G. A.; Fonticelli, M. H.; Carrasco, J.; Carro, P.; Salvarezza, R. C. Alkanethiol Adsorption on Platinum: Chain Length Effects on the Quality of Self-Assembled Monolayers. *J. Phys. Chem. C* **2011**, *115*, 17788−17798.
(25) Heister, K.; Rong, H.-T.; Buck, M.; Zharnikov, M.; Grunze, M.; Johansson, L. S. O. Odd−Even Effects at the S-Metal Interface and in the Aromatic Matrix of Biphenyl-Substituted Alkanethiol Self-Assembled Monolayers. *J. Phys. Chem. B* **2001**, *105*, 6888−6894.
(26) Zharnikov, M. High-Resolution X-Ray Photoelectron Spectroscopy in Studies of Self-Assembled Organic Monolayers. *J. Electron Spectrosc. Relat. Phenom.* **2010**, *178−179*, 380−393.
(27) Corthey, G.; Rubert, A. A.; Picone, A. L.; Casillas, G.; Giovanetti, L. J.; Ramallo-López, J. M.; Zelaya, E.; Benitez, G. A.; Requejo, F. G.; José-Yacamán, M.; et al. New Insights Into the Chemistry of Thiolate-Protected Palladium Nanoparticles. *J. Phys. Chem. C* **2012**, *116*, 9830−9837.
(28) Battocchio, C.; Meneghini, C.; Fratoddi, I.; Venditti, I.; Russo, M. V.; Aquilanti, G.; Maurizio, C.; Bondino, F.; Matassa, R.; Rossi, M.; et al. Silver Nanoparticles Stabilized with Thiols: A Close Look at the Local Chemistry and Chemical Structure. *J. Phys. Chem. C* **2012**, *116*, 19571−19578.
(29) Feulner, P.; Niedermayer, T.; Eberle, K.; Schneider, R.; Menzel, D.; Baumer, A.; Schmich, E.; Shaporenko, A.; Tai, Y.; Zharnikov, M. Strong Temperature Dependence of Irradiation Effects in Organic Layers. *Surf. Sci.* **2005**, *593*, 252−255.
(30) Gonella, G.; Cavalleri, O.; Terreni, S.; Cvetko, D.; Floreano, L.; Morgante, A.; Canepa, M.; Rolandi, R. High Resolution X-Ray Photoelectron Spectroscopy of 3-Mercaptopropionic Acid Self-Assembled Films. *Surf. Sci.* **2004**, *566−568*, 638−643.
(31) Oliveira, J. P.; Keijok, W. J.; Prado, A. R.; Guimarães, M. C. C. Tracking the Effect of Binder Length on Colloidal Stability and Bioconjugation of Gold Nanoparticles. *Appl. Nanosci.* **2018**, *8*, 1781−1790.
(32) Foubert, A.; Beloglazova, N. V.; Hedström, M.; De Saeger, S. Antibody Immobilization Strategy for the Development of a Capacitive Immunosensor Detecting Zearalenone. *Talanta* **2019**, *191*, 202−208.
(33) Premaratne, G.; Niroula, J.; Patel, M. K.; Zhong, W.; Suib, S. L.; Kalkan, A. K.; Krishnan, S. Electrochemical and Surface-Plasmon Correlation of a Serum-Autoantibody Immunoassay with Binding Insights: Graphenyl Surface versus Mercapto-Monolayer Surface. *Anal. Chem.* **2018**, *90*, 12456−12463.
(34) Huang, X.; Chen, J.; Fang, X.; Yan, C.; Shao, H. Exploring the Enhancement of Electron Tunneling Induced by Intermolecular Interactions on Surface of Self-Assembled Monolayer. *J. Electroanal. Chem.* **2019**, *837*, 143−150.
(35) Citrin, P. H.; Wertheim, G. K.; Baer, Y. Core-Level Binding Energy and Density of States from the Surface Atoms of Gold. *Phys. Rev. Lett.* **1978**, *41*, 1425−1428.
(36) Hamelin, A.; Sottomayor, M. J.; Silva, F.; Chang, S.-C.; Weaver, M. J. Cyclic Voltammetric Characterization of Oriented Monocrystalline Gold Surfaces in Aqueous Alkaline Solution. *J. Electroanal. Chem. Interfacial Electrochem.* **1990**, *295*, 291−300.
(37) Grimme, S.; Brandenburg, J. G.; Bannwarth, C.; Hansen, A. Consistent Structures and Interactions by Density Functional Theory with Small Atomic Orbital Basis Sets. *J. Chem. Phys.* **2015**, *143*, 54107.
(38) Neese, F. Software Update: The ORCA Program System, Version 4.0. *Wiley Interdiscip. Rev. Comput. Mol. Sci.* **2018**, *8*, No. e1327.
(39) Heister, K.; Zharnikov, M.; Grunze, M.; Johansson, L. S. O.; Ulman, A. Characterization of X-Ray Induced Damage in Alkanethiolate Monolayers by High-Resolution Photoelectron Spectroscopy. *Langmuir* **2001**, *17*, 8−11.
(40) Petri, M.; Kolb, D. M.; Memmert, U.; Meyer, H. Adsorption of Mercaptopropionic Acid onto Au(1 1 1): Part I. Adlayer Formation, Structure and Electrochemistry. *Electrochim. Acta* **2003**, *49*, 175−182.
(41) Kitagawa, Y.; Hobara, D.; Yamamoto, M.; Kakiuchi, T. Counterion Binding Induces Attractive Interactions Between Negatively-Charged Self-Assembled Monolayer of 3-Mercaptopropionic Acid on Au(111) in Reductive Desorption. *J. Solid State Electrochem.* **2008**, *12*, 461−469.
(42) Shaporenko, A.; Zharnikov, M.; Feulner, P.; Menzel, D. Quantitative Analysis of Temperature Effects in Radiation Damage of Thiolate-Based Self-Assembled Monolayers. *J. Phys.: Condens. Matter* **2006**, *18*, S1677−S1689.
(43) Vela, M. E.; Martin, H.; Vericat, C.; Andreasen, G.; Hernández Creus, A.; Salvarezza, R. C. Electrodesorption Kinetics and Molecular Interactions in Well-Ordered Thiol Adlayers On Au(111). *J. Phys. Chem. B* **2000**, *104*, 11878−11882.
(44) Esplandiú, M. J.; Hagenström, H.; Kolb, D. M. Functionalized Self-Assembled Alkanethiol Monolayers on Au(111) Electrodes: 1. Surface Structure and Electrochemistry. *Langmuir* **2001**, *17*, 828−838.
(45) Kawaguchi, T.; Yasuda, H.; Shimazu, K.; Porter, M. D. Electrochemical Quartz Crystal Microbalance Investigation of the Reductive Desorption of Self-Assembled Monolayers of Alkanethiols and Mercaptoalkanoic Acids on Au. *Langmuir* **2000**, *16*, 9830−9840.
(46) Hobara, D.; Miyake, K.; Imabayashi, S.; Niki, K.; Kakiuchi, T. In-Situ Scanning Tunneling Microscopy Imaging of the Reductive Desorption Process of Alkanethiols on Au(111). *Langmuir* **1998**, *14*, 3590−3596.
(47) Martin, H.; Vericat, C.; Andreasen, G.; Vela, M. E.; Salvarezza, R. C. A Monte Carlo Simulation for the Stripping of the $\sqrt{3}\times\sqrt{3}$ R30° Alkanethiol Lattice from Au(111) Terraces and Steps. *J. Chem. Phys.* **2002**, *117*, 2293−2298.
(48) Vericat, C.; Andreasen, G.; Vela, M. E.; Salvarezza, R. C. Dynamics of Potential-Dependent Transformations in Sulfur Adlayers on Au(111) Electrodes. *J. Phys. Chem. B* **2000**, *104*, 302−307.
(49) Lobo Maza, F.; Méndez De Leo, L.; Rubert, A. A.; Carro, P.; Salvarezza, R. C.; Vericat, C. New Insight into the Interface Chemistry and Stability of Glutathione Self-Assembled Monolayers on Au(111). *J. Phys. Chem. C* **2016**, *120*, 14597−14607.
(50) Zhong, C.-J.; Porter, M. D. Fine Structure in the Voltammetric Desorption Curves of Alkanethiolate Monolayers Chemisorbed at Gold. *J. Electroanal. Chem.* **1997**, *425*, 147−153.
(51) Cometto, F. P.; Ruano, G.; Soria, F. A.; Calderón, C. A.; Paredes-Olivera, P. A.; Zampieri, G.; Patrito, E. M. Thermal and Chemical Stability of N -Hexadecanethiol Monolayers on Au(111) in O 2 Environments. *Electrochim. Acta* **2016**, *215*, 313−325.

DOI: 10.1021/acs.jpcc.9b07271
J. Phys. Chem. C 2019, 123, 24156−24164

(52) Singh, M. S. 4.9 Anion-Stabilizing Groups Allows E1cB. In *Advanced Organic Chemistry: Reactions And Mechanisms*; Always learning; Pearson Education, 2004; p 148.
(53) Carey, F. A.; Sundberg, R. J. 6.6 - The E2, E1 and E1cb Mechanisms. In *Advanced Organic Chemistry: Structure And Mechanisms*; 2000; p 378.

DOI: 10.1021/acs.jpcc.9b07271
J. Phys. Chem. C 2019, 123, 24156−24164